A MULTIBLOCK MULTIGRID THREE-DIMENSIONAL EULER EQUATION SOLVER

Frank E. Cannizzaro Alaa Elmiligui

Old Dominion University, Norfolk, VA

N. Duane Melson
NASA Langley Research Center
Hampton, VA

E. von Lavante
University of Essen
Essen, West Germany

Current aerodynamic designs are often quite complex (geometrically). Flexible computational tools are needed for the analysis of a wide range of configurations with both internal and external flows. In the past, geometrically dissimilar configurations required different analysis codes with different grid topologies in each. The duplicity of codes can be avoided with the use of a general multiblock formulation which can handle any grid topology. Rather than 'hard wiring' the grid topology into the program, it is instead dictated by input to the program.

In the present work the compressible Euler equations, written in a body-fitted finite-volume formulation, are solved using a pseudo-time-marching approach. Two upwind methods (van Leer's flux-vector-splitting and Roe's flux-differencing) have been investigated. Two types of explicit solvers (a two-step predictor-corrector and a modified multistage Runge-Kutta) have been used with multigrid acceleration to enhance covergence.

A multiblock strategy is used to allow greater geometric flexibility. The solution domain is divided into multiple zones (blocks) and the grid for each block is then generated. If the blocks are chosen appropriately, the difficulty of generating a boundary-fitted grid is significantly reduced. Also, the placement of wall boundary conditions is limited only by the placement of the face of a block. The trade-off for this flexibility is the overhead required for the communication between the multiple blocks. In the present multiblock implementation, two simplifying assumptions have been made. First, the interfaces between blocks are assumed to have C^0 continuity. Second, the boundary condition on any face of a block is assumed to be homogeneous across the entire face

(i.e., either completely a wall, an inflow/outflow boundary, or an interface with another block). On block faces that have either a wall or an inflow/outflow boundary condition, 'standard' boundary conditions are used. On faces that are interfaces, a special interface routine presets the values in two ghost cells (normal to the face) equal to the current values in the coincident interior cells in the adjacent block. The updates of the interface ghost cells are performed before each iteration in a given block. The iteration of each block can then proceed without the need for further information from adjacent blocks.

There are two possible strategies for the implementation of multigrid with a multiblock grid structure: (1) multigrid inside of multiblock and (2) multiblock inside of multigrid. With the first strategy, a complete multigrid cycle (or cycles) is (are) performed for a given block. Then work begins on the next block and so forth until all the blocks are complete. This strategy allows the flexibility of different numbers and/or types of multigrid cycles for different blocks, which are adjusted to speed convergence of slowly converging blocks (assuming only steady-state results are sought). Unfortunately, communication between the blocks is reduced. The rate of convergence is reduced. (The interface boundary conditions of the adjacent blocks have to remain fixed in time or a special interface condition has to be used for the blocks to communicate from different multigrid levels).

With the second strategy, multiblock inside of multigrid, all the points on the multigrid fine grid (grid h) in all the blocks are updated before the multigrid process continues to the coarse grid (grid 2h). There, all the points for all the blocks are updated before proceeding to the next coarser multigrid grid. This allows communication between the coarse grids in the multigrid cycle. This method can also identically reproduce the convergence history of a single block solution using an explicit algorithm– a useful debugging tool for the multiblock logic. This latter strategy was used in the present work to compute corner flow through a duct, flow from a jet exhaust mixing with freestream air, and transonic flow over an ONERA M6 wing, without changing the computer program.

1989 Cannizzaro

SIMPLE EXPLICIT UPWIND SCHEMES FOR SOLVING COMPRESSIBLE FLOWS

E. von Lavante
Universität GH Essen, D-4300 Essen, West Germany
A. El-Miligui and F. E. Cannizzaro
Old Dominion University, Norfolk, VA 23508, USA
H. A. Wardh
University of Alexandria, Alexandria, Egypt

SUMMARY

Several upwind numerical methods for solving the compressible inviscid and viscous flow equations are discussed. Due to their explicit nature, the schemes are very simple and easy to apply to solutions on multi-block structured grids. Their favourable high frequence damping results in good rates of convergence when combined with multigrid procedures. The schemes are optimized using a simple stability and damping factor analysis. Results for three-dimensional test cases are shown and discussed. Attention is payed to the relative efficiencies of these schemes.

INTRODUCTION

After several decades of existance, computational fluid dynamics finally matured enough to allow the solving of complex, realistic problems with confidence. Several numerical schemes are in widespread use today, solving variety of compressible, viscous and inviscid problems.

The simple central difference schemes are particularly popular and effective in inviscid flow predictions. The necessity of the addition of ambiguous artificial damping makes them difficult to apply to viscous cases. The typical representatives of these numerical methods is for example the implicit ARC3D code by Pulliam and Steger [1] or the prolific Runge-Kutta (R-K) based explicit schemes as introduced by Jameson, Schmidt and Turkel [2].

The upwind schemes are more complex, but also typically more robust and reliable, especially for viscous computations. They are based on several variation of the Riemann problem solver. Typical examples are the CFL3D code developed by Thomas et. al. [3], based on the Roe's approximate Riemann problem solution and implemented as a flux difference scheme, or the Osher scheme as used by Chakravarthy and Osher [4]. Both of these schemes are implicit. The upwind schemes are usually reported to be better suitable for compressible, viscous predictions than the central difference codes.

The above schemes are very effective in converging to steady states on single-block grids of modest complexity. Most of the currently used schemes are implicit. The implicit formulation allows the use of large time steps, decreasing the number of iterations needed to obtain converged steady state. Due to the simplifications made during the development of these methods (linearization) and the frequent use of explicit boundary conditions, the maximum allowable CFL number has been reported as low as ~3.0 for complicated three-dimensional flows. The implicit part of these solvers also provides effective high frequence damping in connection with the application of multigrid procedures.

The application of the above numerical methods to realistic three-dimensional configurations of significant geometric complexity is usually not possible without the use of multi-block structured (zonal) grids. Here, the computational grid is subdivided into a number of blocks of different size and resolution, either overlapping or non-overlapping. A computational grid of this type adapts much easier to the geometric shape of the bodies as well as flow features. The transfer of information between the blocks is typically carried out explicitely by ensuring the conservation of fluxes accross the block interfaces. The consequence of this procedure is a significant reduction of the maximum allowable CFL number to values between 2. and 5. At these CFL numbers, an explicit upwind scheme of good accuracy when applied to viscous problems and suitable for multigrid procedures seems to offer a better choice.

There is a very large number of explicit schemes that have been used or are still in use for solving the compressible flow equations in their inviscid form (Euler) or viscous form (Navier-Stokes). The numerical method should be simple, efficient, robust, have effective damping of high frequence errors (neccesary for multigrid), have low dispersion (low phase error will reduce spurious oscillations and result in faster convergence rates), low levels of numerical dissipation for accurate predictions of viscous effects and maintain high resolution on stretched grids.

BASIC ALGORITHM

The scheme is based on Roe's flux difference splitting [5,3]. This type of upwind scheme is simplified by linearizing the Riemann problem between two cell interfaces about a state obtained by Roe's averaging procedure, Ref. [5]. The present discretization employed the finite volume approach, with the state variables at the cell interfaces determined by the MUSCL interpolation, using mostly the so-called κ scheme.

In the inviscid case, the governing equations are the three-dimensional Euler equations, expressed in nondimensional conservation law form for curvilinear coordinates ξ, η, ζ , using the usual fluid dynamics notation, as:

$$\frac{\partial Q}{\partial t} + \frac{\partial E}{\partial \xi} + \frac{\partial G}{\partial \eta} + \frac{\partial H}{\partial \zeta} = 0 \qquad (1)$$

$$Q = \begin{bmatrix} \rho \\ \rho u \\ \rho v \\ \rho w \\ \rho E \end{bmatrix} \qquad F = \begin{bmatrix} \rho \hat{U}_\xi \\ \rho \hat{U}_\xi u + p\hat{\xi}_x \\ \rho \hat{U}_\xi v + p\hat{\xi}_y \\ \rho \hat{U}_\xi w + p\hat{\xi}_z \\ \rho \hat{U}_\xi H \end{bmatrix}$$

$$H = E + \frac{p}{\rho} , \qquad E = e + \tfrac{1}{2}(u^2 + v^2 + w^2) , \qquad \hat{t} = \frac{t}{V}$$

$$U_\xi = \hat{\xi}_x u + \hat{\xi}_y v + \hat{\xi}_z w$$

$$\hat{e}^\xi = \frac{\vec{e}^\xi}{J} = V(\vec{\nabla}\xi) = \Lambda_\xi \frac{\vec{e}^\xi}{|\vec{e}^\xi|} = (\hat{\xi}_x , \hat{\xi}_y , \hat{\xi}_z)$$

where Q is the vector of dependent conservative flow variables and F, G and H are the usual flux vectors in the direction ξ, η and ζ, respect. The semidiscrete form of the governing equations is obtained from (1) by carrying out the spatial discretization, assuming $\Delta\xi = \Delta\eta = \Delta\zeta = 1.0$

$$\frac{\partial F}{\partial \xi} \approx F_{i+\frac{1}{2}} - F_{i-\frac{1}{2}} \tag{2}$$

In equation (2), $F_{i+1/2}$ is the numerical flux vector at the cell interface between cells i,j,k and i+1,j,k; i,j,k are the spatial indices in the directions ξ, η and ζ, respectively. The expressions in the other two directions are similar and will not be repeated here. Then,

$$\frac{\partial Q}{\partial t} = R^n_{i,j,k} = (F_{i+\frac{1}{2}} - F_{i-\frac{1}{2}}) + (G_{j+\frac{1}{2}} - G_{j-\frac{1}{2}}) + (H_{k+\frac{1}{2}} - H_{k-\frac{1}{2}}) \tag{3}$$

Following Ref. [5], the numerical flux $F_{i+\frac{1}{2}}$, for example, is evaluated as

$$F_{i+\frac{1}{2}} = \tfrac{1}{2}[F_R + F_L - \tilde{S}_\xi |\tilde{\Lambda}_\xi| \tilde{S}_\xi^{-1} (Q_R - Q_L)] \tag{4}$$

Here, $F_R = F(Q_R)$, $F_L = F(Q_L)$, where Q_R and Q_L are the conservative flow variables describing the states right and left of the cell interface and are obtained by an appropriate interpolation or extrapolation. The last expression in eq. (4) is a damping term due to the upwind character of the present approach; $\tilde{S}_\xi$ and $\tilde{\Lambda}_\xi$ are the eigenvector and eigenvalue matrices of the flux Jacobian matrix $\frac{\partial F}{\partial Q}$, evaluated using the Roe averaged flow variables $\tilde{\rho}$, $\tilde{u}$, $\tilde{v}$, $\tilde{w}$ and $\tilde{h}$, given in [5].

The selection of a particular type of time stepping will determine the characteristics of the numerical method. In the present work, explicit multi-stage schemes were considered; their S-stage version can be written in a somewhat general form as

$$s \le S: \quad Q^s_{i,j,k} = Q^n_{i,j,k} - \alpha_s \Delta t\, \mathcal{F}(R^{s-1}_{i,j,k} , R^{s-2}_{i,j,k} , \ldots R^1_{i,j,k} , R^n_{i,j,k}) \tag{5}$$
$$Q^{n+1}_{i,j,k} = Q^S_{i,j,k}$$

The above formulation of the time stepping procedure applies not only to the modified Runge-Kutta method in [2], but also many other existing schemes. From these infinitely many possible schemes, only a few are suitable for the above flux difference splitting spatial discretization. They were selected by considering the much simplified scalar, linear case of the wave equations.

In order to compare some of the time-stepping procedures (5), the standard Fourier stability analysis of several schemes was carried out, yielding the amplification factor g and the phase error ϕ/ϕ_e for the simple wave equation

$$\frac{\partial u}{\partial t} + c\frac{\partial u}{\partial x} = 0 \quad , \quad c > 0 \tag{6}$$

There are two major blocks of scheme variations that fit eq. (5).

Modified Beam-Warming (BW) Scheme

This scheme was originally introduced by Beam and Warming [6]. It is a two-step method consisting of a first order predictor and second order corrector. It has been slightly modified to make it suitable for the present finite volume formulation:

Predictor:

$$Q_L^1 = Q_i^n \; ; \qquad Q_R^1 = Q_{i+1}^n \tag{7a}$$
$$Q_i^1 = Q_i^n - \Delta t\, R^1$$

Corrector:

$$Q_L^2 = Q_i^n + \tfrac{1}{2}(Q_i^1 - Q_{i-1}^n) \; ; \qquad Q_R^2 = Q_{i+1}^n - \tfrac{1}{2}(Q_{i+2}^n - Q_{i+1}^1) \tag{7b}$$
$$Q_i^2 = Q_i^{n+1} = Q_i^n - \Delta t\, R^2$$

In both steps, only the extrapolations (7a) and (7b) are different; the algebra that completes one iteration, consisting of eq. (3) with (4), is identical. The stability analysis of this scheme is given in every good textbook on CFD and will not be repeated here. The resulting plot of the magnitute of the amplification factor |g| can be seen in Fig. 1a, plotted as a function of the spatial wave number β between 0 and π and the CFL-number σ between 0 and 2.

The scheme is still second order accurate in space and time, satisfies the "shift condition" and has a stability limit of $\sigma=2$. It has a relatively modest dissertion. It was named the "1-2 BW scheme". It is a very simple and efficient method, consisting of only two steps. It performed well on single grids, in particular when applied to unsteady flow predictions.

There were, however, some problems with this scheme. Since the two steps are different, the steady state result will depend on the time step. This phenomen was observed in only a few cases, represented by convergence to residual that was larger than "machine zero". At this time, none of the flux limitors tested in this scheme converged more than two orders of magnitude. The resulting flow fields agreed well with other, fully converged numerical results. This type of behaviour has been observed by other investigators, but is still disturbing.

A more serious problem is the increase of the damping factor to 1.0 at high frequency and $\sigma=1$. In scalar case, the CFL number can be kept at its optimum value (1.7 in the case of the 1-2 BW scheme), but in the case of the Euler equations there are three distinc eigenvalues in each direction. Typically, local time stepping will be implemented, where each cell will be advanced at its optimum time step, corresponding to the maximum eigenvalue at that cell. This means that only the maximum eigenvalue will correspond to the optimum CFL number for high frequence damping and one or more might correspond to the CFL number ranges with very little damping. This was

manifested by the lack of convergence of the 1-2 BW scheme when utilized in a Multi-Grid procedure. For multigrid applications, this scheme was modified by making the first step (predictor) also second order accurate:

$$Q^1_{i,} = Q^n_i + \tfrac{1}{2}(Q^n_i - Q^n_{i-1}) \; ; \qquad Q^1_{it} = Q^n_{i+1} - \tfrac{1}{2}(Q^n_{i+2} - Q^n_{i+1}) \tag{8}$$

The plot of the damping characteristics of this scheme, called 2-2 BW, is shown in Fig. 1b. The maximum stable CFL number is now only 1.0, but the high frequence damping is much better. This scheme worked well with Multi-Grid and will be discussed below.

Modified Runge-Kutta Methods

The modified R-K methods, with the standard set of coefficients, have been rather successfull in combination with the central difference spatial discretization. They have been, however, performing very poorly with upwind differencing. The standard coefficients have to be modified to achieve better performance, resulting in schemes that are in general of reduced accuracy in time. In order to find the optimum sets of the R-K coefficients, a Fourier stability analysis was carried out, similar to the approach in [2]. The extrapolation of the state variables to the cell interfaces was based on the so called κ-scheme:

$$Q^s_{i,} = Q^{s-1}_i + \tfrac{1}{4}\ell^{s-1}_i[(1 - \kappa\ell_i)\Delta_i + (1 + \kappa\ell_i)\Delta^+_i]^{s-1} \; ; \tag{9a}$$

$$\Delta_i = Q_i - Q_{i-1} \; ; \qquad \Delta^+_i = Q_{i+1} - Q_i \; ; \tag{9b}$$

$$Q^s_{it} = Q^{s-1}_{i+1} - \tfrac{1}{4}\ell^{s-1}_{i+1}[(1 + \kappa\ell_{i+1})\Delta_{i+1} + (1 - \kappa\ell_{i+1})\Delta^+_{i+1}]^{s-1} \; ; \tag{9c}$$

where ℓ is one of the possible flux limitors. The value of the parameter κ determines the spatial accuracy of the scheme; $\kappa=-1$ is fully upwind, second order accurate; $\kappa=0$ is the upwind biased second order Fromm scheme; $\kappa=\frac{1}{3}$ is upwind biased third order and $\kappa=1$ is second order central difference scheme. The first order scheme is obtained by setting $\ell=0$. In the present stability analysis, the limitor ℓ was set to 1 (no limitor) for simplicity.

The R-K time stepping for equation (6) can be written as

$$u^s = u^n - \alpha_s \, \Delta t \, R^{s-1} \; ; \qquad R^s = \frac{\partial(cu^s)}{\partial x} \tag{10}$$

Here, $\alpha_S=1$ for consistancy, with $u^{n+1} = u^S$. Making the assumption that u is harmonic, leads to

$$-R = -c\frac{\partial u}{\partial x} = \frac{\partial u}{\partial t} = u_0 z e^{zt} = zu \tag{11}$$

Defining $P=\Delta t\, z$, substituting eq. (11) in eq. (10) and some simple algebra yields

$$g = (u^{n+1}/u^n) = 1 + P + \alpha_{S-1}P^2 + \ldots + \alpha_1\alpha_2\ldots\alpha_{S-1}P^S \tag{12}$$

Clearly, for stability, $\Re(P)<0$ and $|g|\le 1$. The stability and damping properties of the scheme are associated with the complex polynomial (12). The damping $|g|$ is a function of the complex $P=x+Iy$, $I=\sqrt{-1}$, and can be best shown as a plot of contours of constant $|g|$ between 0 and 1. However,

$$u_i = u|_{x=I\Delta x} = \hat{u}_0 e^{I\beta i} \tag{13}$$

where β is the spatial wave number, ranging from 0 to π. Values of β between $\frac{\pi}{2}$ and π are considered high frequencies. P now represents the Fourier transform of the spatial differencing operator and can be superimposed on the damping factor contour plots. Defining

$$\sigma = \frac{c\Delta t}{\Delta x} \tag{14}$$

as the CFL number, and observing that $F_{i+\frac{1}{2}}=cu_{i+\frac{1}{2}}$ gives

$$R = -zu = \frac{1}{\Delta x} c(u_{i+\frac{1}{2}} - u_{i-\frac{1}{2}}) \tag{15}$$

Eq. (15), combined with eq.(13) and (9), for $\ell=1$, yields finally

$$P = -\sigma(1-e^{-i\beta})(1 + \frac{1-\kappa}{4}(1-e^{-i\beta}) - \frac{1+\kappa}{4}(1-e^{i\beta})) \tag{16}$$

P is a function of σ and β; the plot of $P(\sigma,\beta)$ and $|g|$ can be used to optimize the coefficients α_s. The resulting stability plots are shown only in the upper half of the negative real part of P (fourth quadrant) since they are symmetric with respect to the y=0 coordinate line. The optimization of the coefficients α_s was carried out by displaying these stability plots on a PC-type microcomputer. The changes in the shape of the $|g|$ contours were observed in real time as the coefficients were changed. The "islands" of the low value of $|g|$ correspond to the roots of the polynomial (12). The main purpose of this optimization was to find a combination of the coefficients α_s such that, for as large σ as possible, there would be good high frequency damping (low value of $|g|$) for a large range of σ (maximum size of the "islands" as close to the real axis as possible). The optimization was performed for four different spatial discretizations (1-st order; 2-nd order fully upwind, $\kappa=-1$; 2-nd order Fromm scheme, $\kappa=0$; 3-rd order upwind bias, $\kappa=\frac{1}{3}$) for the two-, three- and four-stage R-K schemes. Even in the case of the four-stage scheme, the actual optimization of the three coefficients ($\alpha_S=1$) was relatively easy and quick, once the influence of the coefficients on the stability plots was understood. Only a few selected stability plots of the most interesting schemes will be presented here. The optimized coefficients are summarized in Table 1.

The simplest schemes to optimize were all the two-stage versions, since only one coefficient is freely selectable. The case of $\kappa=0$ is shown in Fig. 2a. For the optimum coefficient $\alpha_1= 0.42$, the theoretically determined maximum stable cfl number was 1. The Fromm scheme performed very well in most of the test cases due to its very low numerical dispersion.

The four-stage R-K schemes are more interesting. Here, the optimum combination of three coefficients has to be found. The standard R-K coefficients ($\alpha_1=\frac{1}{4}$; $\alpha_2=\frac{1}{3}$; $\alpha_3=\frac{1}{2}$; $\alpha_4=1$), shown in Fig. 2b for the third-order scheme, performend, as expected, relatively poorly. It should be noted that, when multi-grid procedures are implemented, the maximum CFL-number is of little importance. The high frequency damping (or lack of it) will effect the rate of convergence to steady state more significantly than the CFL-number. In this case of standard coefficients, the maximum stable CFL number is relatively low at $\sigma=1.7$, but, more significantly, the damping of high frequencies of error propagation (at $\beta>\frac{\pi}{2}$) is very weak. The result of the present optimization, shown in Fig. 2c, is much more promissing.

It should be mentioned here that, in a parallel effort, van Leer et. al. [7] also tried to optimize the R-K coefficients for applications with the upwind methods. Their approach was somewhat different: assuming that a genuine and practical multi-dimensional characteristic formulation of the Euler equations could be found, they optimized the R-K coefficients for only one value of σ, argueing that each wave would be propagated at its optimum CFL-number. Unfortunately, there no such formulation for the three dimensional case. The advantage of this approach was that the selection

process could be automated, eliminating the "guessing game" involved in the present approach. Their results are shown in Fig. 3b and 3c. Generally, their maximum σ was lower, and the damping effective over a narrower range of CFL values.

In the case of the third order scheme, the present optimum α-s are shown in Fig. 3d. In the real test cases, however, the van Albada limitors were implemented, shifting the P-curve to the left. The real optimum CFL number was therefore much lower (1.8). A new set of coefficients for the limited case was found. It is shown in Fig. 3e (α_1=.11; α_2=.245; α_3=.48); the maximum σ was 2.5.

RESULTS

Most of the above schemes were tested on number of two- and three-dimensional cases. In general, the optimum CFL numbers agreed well with the above theory. In supersonic cases, the real optimum CFL number was usually somewhat higher; in transonic cases, it was mostly the same.

Due to the space limitations of this paper, only one three-dimensional case will be discussed. Here, the supersonic flow in a channel with two 10^0 compression ramps, at the bottom and left vertical walls, with an inflow Mach number of 3.17, formed a conical shock flow with two Mach tripple points. The resulting flow field, obtained by the Fromm scheme, is shown in Fig. 3. The computations were carried out using a 32x32x32 body fitted grid. The Full-Multi-Grid procedure (FMG) was used with three grid levels with two iterations on each grid level. Considering the results of the above stability analysis, the most promissing schemes of practical importance were the four-stage Fromm scheme (κ=0) and the third order biased scheme ($\kappa=\frac{1}{3}$). The Fromm scheme was preferred due to its low numerical dispersion, demonstrated by results with the least oscillations (no limitors). The convergence of the κ=0 scheme with α_1=.11, α_2=.255, α_3=.46 for different CFL-numbers is shown in Fig. 4. The best rate of convergence was achieved at CFL numbers between 2.0 and 2.3, which was in a surprising agreement with the theory. This scheme, at a σ=2.0, is compared with the simple 2-2 BW scheme at its maximum σ=1.0 in Fig.5. The 2-2 BW scheme seems to be much slower, but it is only a two-stage scheme and thus needs only about half the CPU time per one iteration. Consequently, it is approximately 50% less efficient.

Finally, the present κ=0 scheme is compared with the optimized version of the $\kappa=\frac{1}{3}$ scheme in Ref. [7], used at the optimum CFL number of 1.732. Its performance is much worse, since only one of the three eigenvalues corresponds to the optimum damping case. The application of the van Albada limitor lead to a limit cycle with no apparent convergence. This problem has been reported by other investigators but was still disapointing, since all the two-dimensional cases converged with the limitor in effect. The problem is being further investigated.

CONCLUSIONS

The present study investigated several types of explicit upwind schemes for solving the compressible flow problems. The simple 1-2 BW scheme seems to be very effective for predicting unsteady flows, but it does not work with Multi Grid due to its insufficient damping of high

frequencies at wide range of CFL numbers. The most promissing schemes for Multi-Grid computations are multi-stage R-K methods with optimized sets of coefficients. Here, versions with coefficients optimized for wider range of CFL numbers seem to be more robust than specialized versions. The $\kappa=0$ and $\kappa=\frac{1}{3}$ schemes were successfully tested on several two-dimensional cases and subsequently included in a multi-block, multi-grid code used for predictions of complex three-dimensional flows.

ACKNOWLEDGMENTS

This work was partially funded by NASA Langley Research Center Grant NAG-1-633. The authors would like to thank Mr. M. Salas, Mr. R. Gaffney and Dr. B. van Leer for their comments.

REFERENCES

[1] Pulliam, T.H., and Steger, J.L., "Recent Improvements in Efficiency, Accuracy and Convergence for Implicit, Approximate Factorization Algorithms", AIAA paper 85-0360.

[2] Jameson, A., Schmidt, W. and Turkel, E., "Numerical Solutions of the Euler Equations by Finite Volume Methods Using Runge-Kutta Time-Stepping Schemes", AIAA paper 81-1259.

[3] Thomas, J.L., van Leer, B. and Walters, R.W., "Implicit Flux-Split Schemes for the Euler Equations", AIAA paper 85-1680.

[4] Chakravarthy, S.R. and Osher, S., "Numerical Experiments with the Osher Upwind Scheme for the Euler Equations", AIAA Journal, Vol. 21, Sept. 1983, pp. 1241-1248.

[5] Roe, P.L., "Approximate Riemann Solvers, Parameter Vectors, and Difference Schemes", Journal of Comp. Physics, Vol. 43, 1981, pp. 357-372.

[6] Beam, R.M. and Warming, R.F., "An Implicit Finite-Difference Algorithm for Hyperbolic Systems in Conservation Law Form", Journal of Comp. Physics, Vol. 22, 1976, pp. 87-110.

[7] van Leer, B., Tai, Ch. and Powell, K.G., "Design of Optimally Smoothing Multi-Stage Schemes for the Euler Equations", AIAA paper 89-1933.

Table 1.: Optimum R-K coefficients.

	1-O	$\kappa=-1$	$\kappa=0$	$\kappa=1/3$	
α_1	0.22	0.22	0.42	0.40	2-Stage
α_1	0.105	0.15	0.21	0.22	
α_2	0.325	0.40	0.44	0.48	3-Stage
α_1	0.056	0.091	0.11	0.135	
α_2	0.152	0.24	0.255	0.26	
α_3	0.34	0.42	0.46	0.44	4-Stage

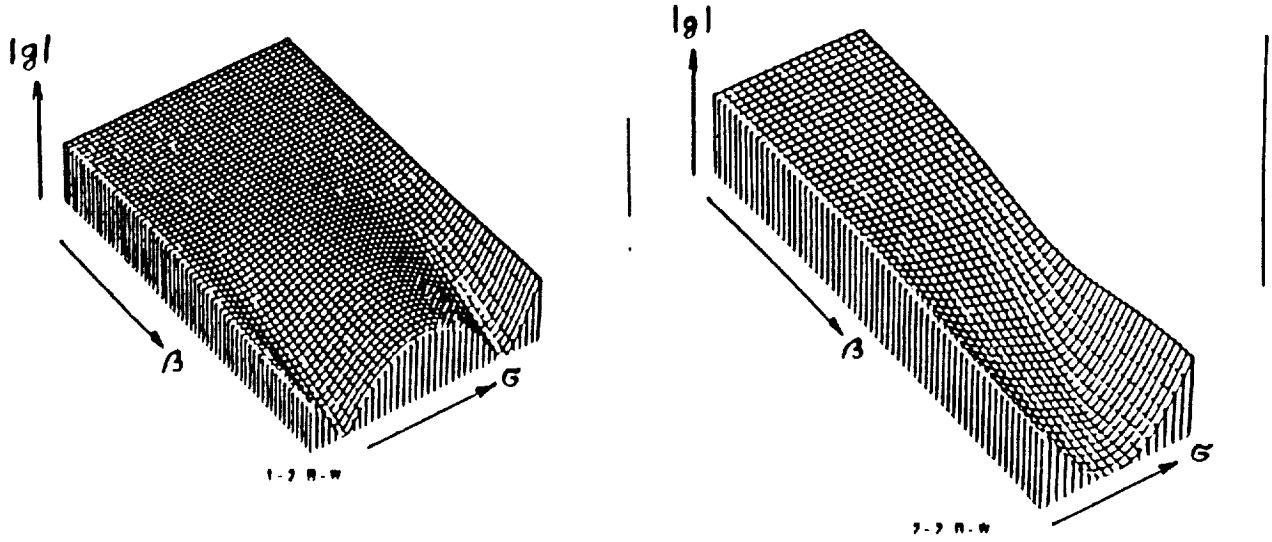

1a) 1-2 BW Scheme

1b) 2-2 BW Scheme

Fig. 1: Amplification factor g as a function of CFL-number and wave number.

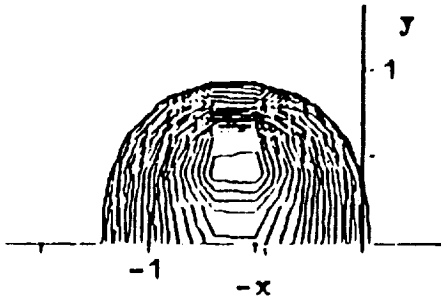

2a) 2-Stage, 2-nd order Fromm, CFL = 1.0

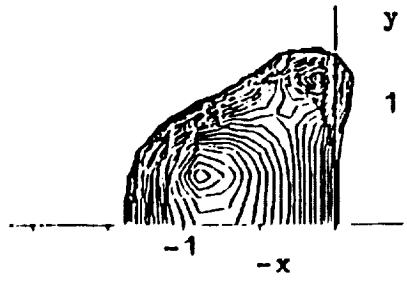

2b) 4-Stage, standard R-K, 3-rd order, CFL = 1.7

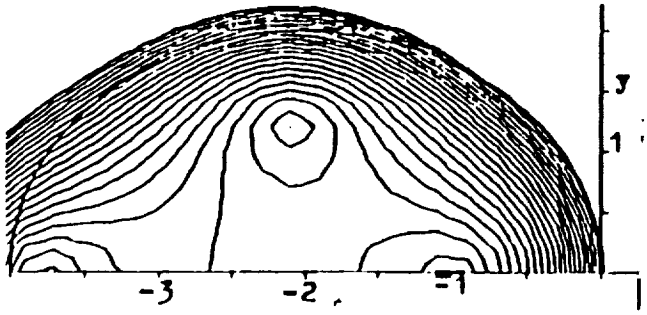

2c) 4-Stage, present optimum, 1-st order, CFL = 4.0

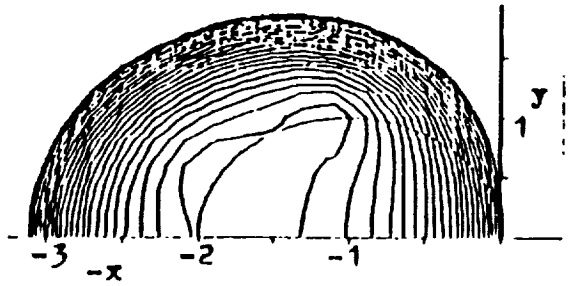

2d) 4-Stage, Ref. 7, optimum, 1-st order, CFL = 2.0

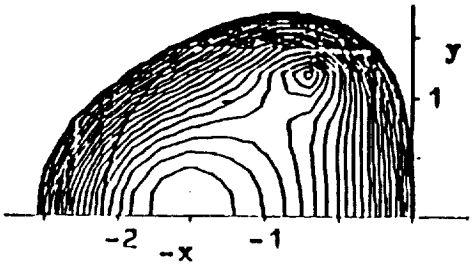

2e) 4-Stage, present optimum, 2-nd order Fromm, CFL = 2.2

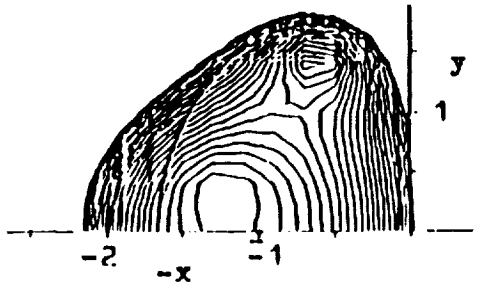

2f) 4-Stage, present optimum, 3-rd order, CFL = 2.5

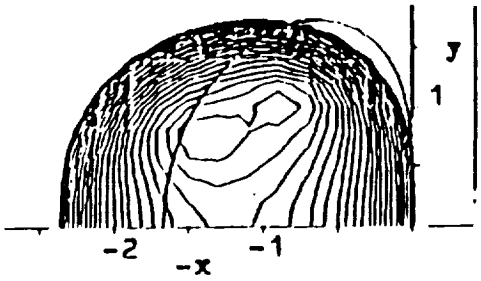

2g) 4-Stage, best w. limitor 3-rd order, CFL = 2.5

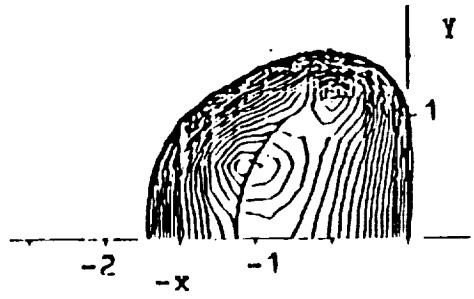

2h) 4-Stage, Ref. 7, optimum 3-rd order, CFL = 1.732

Fig. 2: Stability plots; contours of const. $|g|$ with a trace of P corresponding to a maximum CFL-number.

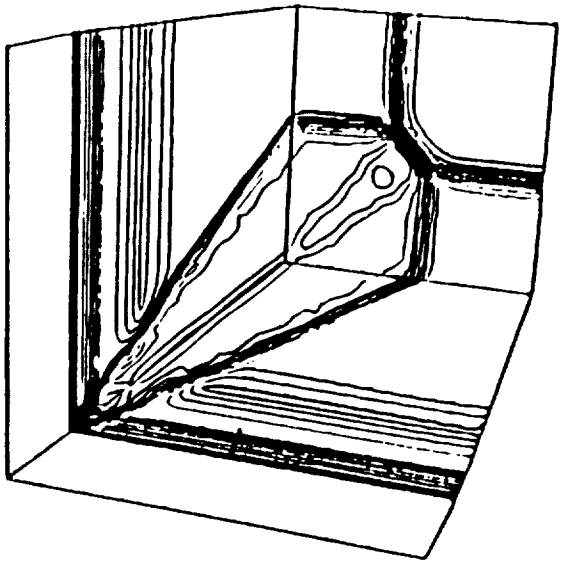

Fig. 3: Mach number contours for corner flow, $M_{in} = 3.17$

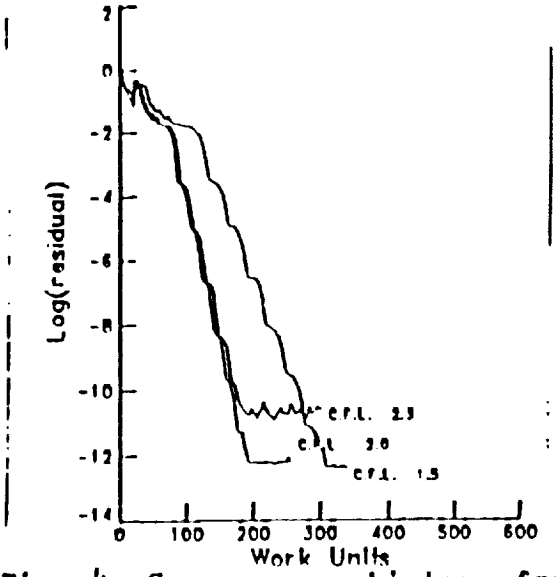

Fig. 4: Convergence history for corner flow, 4-Stage Fromm scheme.

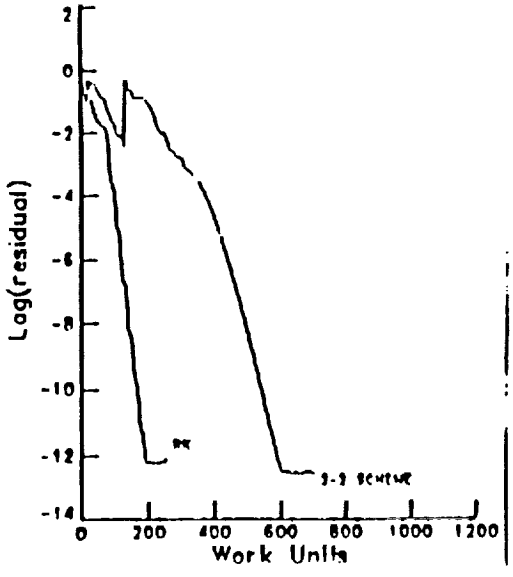

Fig. 5: Comparison of convergence histories for corner flow

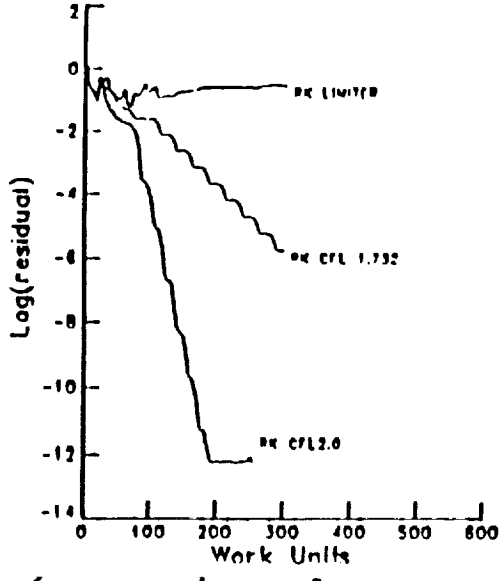

Fig. 6: Comparison of convergence histories for corner flow